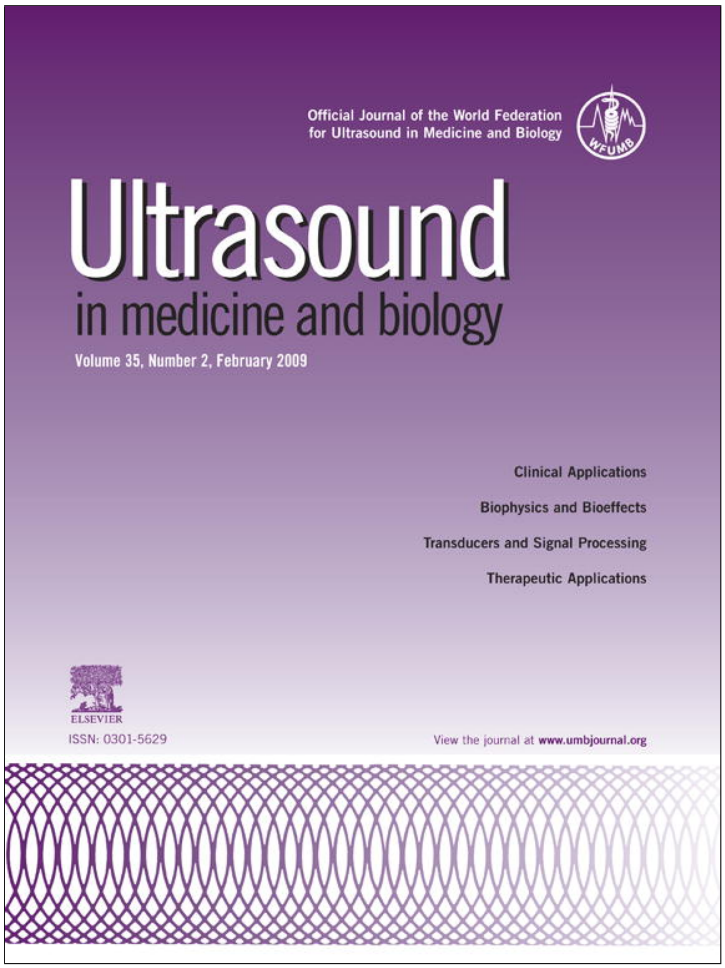

Ultrasound in Med. & Biol., Vol. 35, No. 2, pp. 219–229, 2009

0301-5629/09/$–see front matter

ELSEVIER

doi:10.1016/j.ultrasmedbio.2008.08.018

● *Original Contribution*

QUANTITATIVE VISCOELASTICITY MAPPING OF HUMAN LIVER USING SUPERSONIC SHEAR IMAGING: PRELIMINARY *IN VIVO* FEASABILITY STUDY

Marie Muller, Jean-Luc Gennisson, Thomas Deffieux, Mickaël Tanter and Mathias Fink

Laboratoire Ondes et Acoustique, ESPCI, CNRS UMR 7587, INSERM, Université Paris VII, Paris Cedex 05, France

(*Received* 16 *May* 2008; *revised* 11 *August* 2008; *in final form* 24 *August* 2008)

Abstract—This paper demonstrates the feasibility of *in vivo* quantitative mapping of liver viscoelasticity using the concept of supersonic shear wave imaging. This technique is based on the combination of a radiation force induced in tissues by focused ultrasonic beams and a very high frame rate ultrasound imaging sequence capable of catching in real time the transient propagation of resulting shear waves. The local shear wave velocity is recovered using a dedicated time-of-flight estimation technique and enables the 2-D quantitative mapping of shear elasticity. This imaging modality is performed using a conventional ultrasound probe during a standard intercostal ultrasonographic examination. Three supersonic shear imaging (SSI) sequences are applied successively in the left, middle and right parts of the 2-D ultrasonographic image. Resulting shear elasticity images in the three regions are concatenated to provide the final image covering the entire region-of-interest. The ability of the SSI technique to provide a quantitative and local estimation of liver shear modulus with a millimetric resolution is proven *in vivo* on 15 healthy volunteers. Liver moduli extracted from *in vivo* data from healthy volunteers are consistent with those reported in the literature (Young's modulus ranging from 4 to 7.5 kPa). Moreover, liver stiffness estimation using the SSI mode is shown to be fast (less than one second), repeatable (5.7% standard deviation) and reproducible (6.7% standard deviation). This technique, used as a complementary tool for B-mode ultrasound, could complement morphologic information both for fibrosis staging and hepatic lesions imaging (E-mail: jl.gennisson@espci.fr).

Key Words: **Transient elastography, Ultrasound, Liver fibrosis, Shear wave imaging.**

INTRODUCTION

Liver fibrosis staging is of major clinical issue because it represents key information regarding the prognosis and the surveillance of chronic liver diseases such as cirrhosis or hepatitis. It is also crucial to monitor the efficacy of antifibrotic treatments (Pinzani et al. 2005; National Institute 2002). Currently, liver biopsy and histologic testing remains the gold standard for liver fibrosis staging (Afdhal et al. 2003; Bravo et al. 2001; Ishak et al. 1995). However, this technique presents serious limitations. Its invasive characteristics can lead to patient discomfort and serious complications, especially if repeated biopsies are needed (Bravo et al. 2001; Friedman et al. 2003; Cadranel et al. 2000; Castera et al. 1999). Furthermore, this liver investigation method shows serious deficiencies, mainly related to the fact that fibrosis affects the liver tissue in a heterogeneous manner, leading to sampling errors during punction (Regev et al. 2002; Maharaj et al. 1986) and inter-observer variability during the histopathological measurements (The French METAVIR 1994; Bedossa et al. 1988). To circumvent these limitations, noninvasive biochemical and hematologic tests (Wai et al. 2003), as well as tests measuring the presence of surrogate serum fibrosis markers, have been developed (Suzuki et al. 2005; Patel et al. 2003). Blood tests such as Fibrotest (Imbert-Bismut et al. 2001) and platelet count (Ono et al. 1999) measure a combination of various blood parameters considered as indirect markers of fibrosis staging. The sensitivity and specificity of these tests, measuring items having no direct link with fibrosis, are still debated (Bataller et al. 2005). The accuracy of

Address correspondence to: Jean-Luc Gennisson, LOA – ESPCI, 10 rue Vauquelin, 75231 Paris Cedex 05 France. E-mail: jl.gennisson@espci.fr

their results could indeed be impaired by extra hepatic diseases such as systemic inflammatory phenomena (Stauber et al. 2007; Beaugrand et al. 2006). As far as imaging methods are concerned, magnetic resonance imaging (MRI) has been reported to show satisfying sensitivity and specificity (Aguirre et al. 2006), thus being a useful tool for biopsy guidance (Konig et al. 2004), but MRI, as well as computed tomography and ultrasonic imaging, seem to be unable to determine early stages of fibrosis (Klatt et al. 2006).

Elasticity imaging is now commonly accepted as a relevant tool for soft tissue characterization (Sarvazyan et al. 1998; Ophir et al. 1991) in general, and for the liver in particular (Yeh et al. 2002). The feasibility of MR-elastography for liver fibrosis staging has been recently demonstrated (Klatt et al. 2006; Huwart et al. 2006), but the costs at stake are too large to allow screening or monitoring applications. Another technique, based on 1-D transient elastography (Fibroscan©) has been proposed for the noninvasive staging of liver fibrosis. With this technique, the assessment of fibrosis degree is based on the estimation of a global shear elasticity along an ultrasonic A-line (Sandrin et al. 2003). Various studies have shown a correlation between the liver shear modulus measured using Fibroscan© and the degree of fibrosis obtained through liver biopsy, particularly when the elasticity measurement is combined with a blood marker of fibrosis (Beaugrand et al. 2006; Castera et al. 2005; Saito et al. 2004). However, the Fibroscan© technique estimates a mean elasticity of the liver (over a centimetric volume), and the heterogeneities of shear elasticity at higher fibrosis degree are assumed to introduce biases in this global estimation. Thus, the clinical interest of 2-D real-time elasticity imaging modality would be twofold. First, the estimation of the global liver stiffness over a larger area should result in more accurate scores of fibrosis level. Second, beyond fibrosis staging, the quantitative mapping of local stiffness heterogeneities should allow the localization of the presence of hepatic lesions both for diagnosis and biopsy guidance. Some techniques have been developed that measured the deformation of the liver tissue before and under static compression (Friedrich-Rust et al. 2007). Unfortunately, such static elastography techniques do not allow a quantitative evaluation of the liver elasticity. Another technique based on the use of a local acoustic radiation force impulse (ARFI) technique has been proposed recently for the visualization of abdominal lesions on the liver and the kidney (Fahey et al. 2008; Palmeri et al. 2008). In this approach, 2-D elastography images are obtained by combining successive sequences of ultrasonic radiation forces, each radiation force sequence enabling the estimation of elasticity along one line of the final image. However, this technique requires an important number of insonifications to build a complete elasticity image of the medium and is consequently sensitive to respiratory motion artefacts (Fahey et al. 2006, 2007).

In the study presented here, a 2-D real-time and freehand elastography method is proposed for liver investigation as a multiparametric technique. This approach, called supersonic shear imaging, tries to merge the advantages of the previous techniques by combining the remote palpation of the acoustic radiation force imaging technique (Palmeri et al. 2008) and the ultrafast echographic imaging approach of transient elastography into a single ultrasonic sequence (lasting less than several tens of milliseconds). This combination is expected to provide a quantitative elasticity imaging mode, with a significant reduction of operator dependence compared with static elastography. First, the global estimation of the liver elasticity is performed over a large area to reduce sampling errors and enable the recovery of a global mean elasticity of liver that benefits from very small variance. Second, the local estimation of the liver elasticity is conducted, allowing the mapping of local stiffness heterogeneities. Third, in addition to elasticity, other parameters are assessed such as the dispersive behavior of the liver, by exploiting the frequency diversity of the shear waves propagating in the liver.

In the following, the SSI technique used in this study is presented and the methods for global and local elasticity estimation are presented, as well as the method used for the shear wave dispersion measurements. Finally, *in vivo* reproducibility and repeatability results are presented, as well as measurement on a group of 15 healthy volunteers.

MATERIALS AND METHODS

All subjects were informed of the nature and aims of this study. They signed an informed consent form and the study was approved by the national agency for health (AFSSAPS); authorization # 2008-A00006–49.

Supersonic shear imaging technique

The SSI technique is a tissue elasticity imaging technique based on the velocity estimation of a shear wave generated by radiation force. This technique has been described in previous papers (Bercoff et al. 2004a, 2004b, 2004c; Tanter et al. 2008) and is currently being tested clinically on breast lesion imaging with promising results. A remote radiation force or "pushing beam" is generated by focusing ultrasound using a conventional ultrasonic probe. This radiation force results in a few micrometers displacement of tissue that propagates as a transient shear wave in the medium. By successively focusing multiple beams at increasing depths, a quasi-plane shear wave can be generated. After the generation

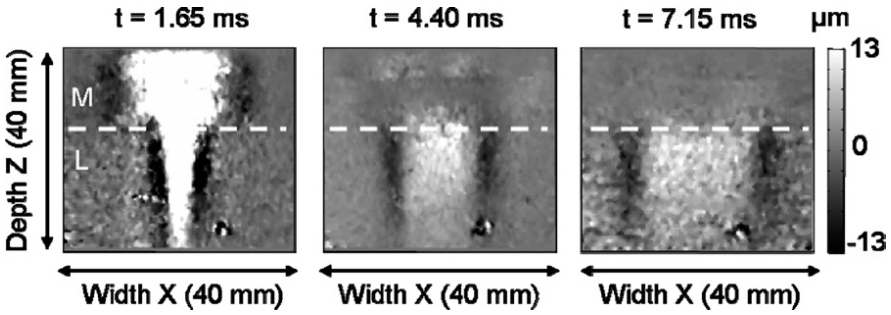

Fig. 1. Shear displacement field in the liver at different time steps. A quasi-plane shear wave is visible, travelling faster in the intercostal muscle region (M) than in the liver region (L). Gray scale levels are expressed in μm, corresponding to local tissue displacement between two successive images (at a 3750-Hz frame rate).

of the shear wave, the echographic device switches to the ultrafast imaging mode by acquiring raw radiofrequency (RF) data at a very high frame rate (up to 5000 frames/s) using the same ultrasonic probe. Each ultrafast echographic image is achieved by transmitting a single ultrasonic plane wave and beamforming only in the receive mode in postprocessing. Then by using a 1-D cross-correlation algorithm, consecutive ultrasonic images were compared to determine the axial displacement field U (along the Z axis) induced by the propagation of the shear wave inside the tissues (Fig. 1).

In these *in vivo* investigations, the SSI technique was implemented on a modified commercial ultrasonic scanner HDI 1000 (ATL, Seattle, WA, USA) with a 5-MHz linear probe (L7.4, ATL, 5 MHz central frequency, 128 elements). The shear wave was generated by successively focusing four 5-MHz ultrasonic beams 20, 25, 30 and 35 mm deep. Each pushing beam lasted 150 μs, with a f/day number of 1.5. The following ultrafast echographic mode was performed at 3750 Hz frame rate, with 128 successive ultrafast echographic images. As the HDI 1000 scanner is only relying on 32 receive channels (and 64 transmit channels), the ultrafast echographic frame is achieved by transmitting four successive plane waves with 32 elements of the probe. The duration of each transmit/receive event (about 50 μs) is only limited by the ultrasonic travel path and, consequently, the maximal imaging depth fixed between 0 and 37 mm. A complete ultrasound image, comprising 128 lines spaced at 0.3 mm (space between each elements of the probe), is thus achieved in the minimum duration of 200 μs with this scanner. The whole SSI acquisition itself corresponds to a total duration of about 25 ms with 128 images recorded; however, a 200-ms pause automatically follows each acquisition.

Regarding the FDA requirements, the acoustic pressure levels and intensities were measured using a calibrated MHB 500B (NTR systems, 0.5 mm resolution, frequency bandwidth ranging from 1 to 16 MHz). The peak pressure measured at 2 cm depth in the water was 4 MPa; this pressure must be corrected inside the tissue by an attenuation of 0.3 dB/cm/MHz, leading to a peak pressure of $p_0 = 2$ MPa inside the tissue (at $f_0 = 5$ MHz). The Ispta is defined as:

$$Ispta = \frac{p_0^2}{2\rho_0 c} \cdot \frac{\Delta t_{push}}{\Delta t_{experiment}}. \quad (1)$$

Considering the "worst cases" where all four pushing beams are focused at the same location, $\Delta t_{push} = 4*150 = 600$ μs in $\Delta t_{experiment} = 225$ ms, the *Ispta* would be 591, 447, 306 and 239 mW/cm^2, respectively, at focal depths z = 20 mm, z = 25 mm, z = 30 mm and z = 35 mm. Note that all these "worst cases" values corresponding to insonifications, which were never used *in vivo*, are below the 720mW/cm^2 510(k) recommendation imposed by the FDA. The *Ispta* value corresponding to the case used for *in vivo* investigations (four successive "pushes" each lasting 150 μs and focused at z = 20, 25, 30 and 35 mm) is equal to 395 mW/cm^2. The mechanical index for the pushing sequence was found to be, respectively, 1.42, 1.3, 1.15 and 0.95 for z = 20, 25, 30 and 35 mm depth and 0.67 for the ultrafast imaging sequence, also below the 1.9 limit imposed by the FDA.

In vivo shear waves displacements are represented in Fig. 1 at different time steps after the radiation force generation. One can clearly notice the quasi-planar shear wave front propagating faster in the upper region of the image corresponding to the intercostal muscle. The intercostal muscle (M), usually stiffer than the liver (L), exhibits a higher shear velocity. In Figs. 1 and 2, one can also notice large vessels (circular shapes in the bottom of the images) where the displacement field uncorrelated because of the presence of fluid and, consequently, a lack of echogenicity.

Moreover, to investigate a larger region of the liver and to increase the shear velocity estimation zone by zone, three quasi-plane shear waves were successively generated in three different locations of the image. This

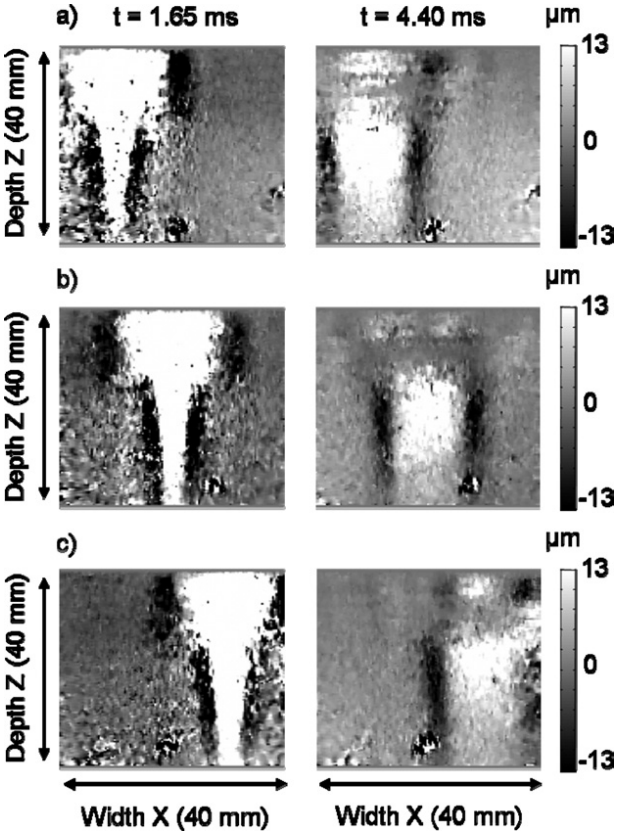

Fig. 2. Displacement field at two times (t = 1.65 ms and t = 4.40 ms) for three different locations: right (a), center (b) and left (c) of the echographic image. The shear wave then propagates both ways from the push location. For each location of the pushing beam, a movie of the displacement is recorded to investigate the full imaged area of the liver. Grayscale levels are expressed in μm, corresponding to local tissue displacement between two successive images (at a 3750-Hz frame rate).

results in a set of three different movies of the same liver region presented on Fig. 2, from which shear velocity can be estimated.

From these quasi-plane shear wave propagation movies, three different kinds of information can be extracted.

An elasticity map

The local estimation of the shear wave group velocity enables the creation of an elasticity map of the liver *via* the classical relation $E = 3\rho c^2$, where ρ is the local tissue density (assumed to be constant and equal to 1000 kg.m–3), c is the shear wave group velocity and E is the Young's modulus (Royer and Dieulesaint 2000). For each pixel (z,x), the local shear group velocity c is estimated *via* a time-of-flight algorithm, which computes the delay dt between two points separated from a distance dx through cross correlation.

$$U\left(x - \frac{dx}{2}, z, t\right) = s(t) \tag{2}$$

and

$$U\left(x + \frac{dx}{2}, z, t\right) = s(t + dt), \tag{3}$$

where U is the displacement field, dx the distance between the two points used, s is the signal waveform and dt is the time delay between the two points. Multiple distances dx can be used to provide multiple estimations of the shear velocity ($c = dx/dt$) at the same pixel and improve the overall quality of the measurement through averaging. The maximum distance dx chosen for the shear wave group velocity estimation sets the resolution of the map.

A global elasticity score

From a large region-of-interest (ROI) chosen in the image (typically 30 × 40 mm^2), a single estimation of the elasticity can be estimated. This global estimation relies on the use of multiple separation distances dx (dx values chosen not to exceed the ROI) for the shear wave group velocity estimation, as well as averaging inside the ROI. This ROI is chosen from the B-mode image to avoid the intercostal muscle or fat present in the upper region, as well as to avoid the pushing area itself (Fig. 3a); a histogram of the estimated shear velocity is also represented (Fig. 3b). This enables the assessment of a global elasticity value with a smaller variance adapted for liver staging. Similar to 1-D transient elastography provided by Fibroscan©, this 2-D global elasticity value can be seen as a score for fibrosis staging.

A complete rheological analysis using shear wave spectroscopy

A more detailed analysis of the semilocal shear mechanical behavior of the liver can be performed using

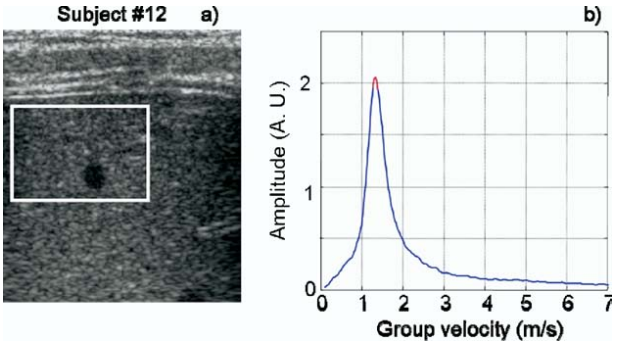

Fig. 3. (a) Standard B-mode image of the liver of a healthy volunteer. In the upper part, the intercostal muscle is clearly visible. (b) Group velocity estimation estimated from the ROI (white rectangle). The maximal value of the histogram corresponds to a shear wave group velocity equal to 1.37 m/s.

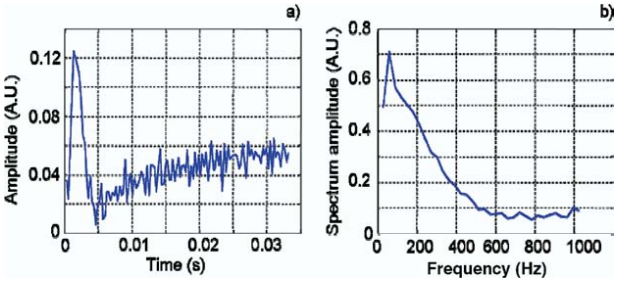

Fig. 4. (a) Amplitude in arbitrary unit (*A.U.*) of the shear displacement as a function of time. The tissue velocity wave field is visible after 5 ms. (b) Spectrum of the shear wave displacement field in arbitrary unit (*A.U.*). The signal is clearly broadband and the signal-to-noise ratio is well defined between 50 Hz and 400 Hz.

the shear wave spectroscopy technique as described by Deffieux et al. (2008). This last approach corresponds to the determination of shear wave phase velocity dispersion over a large frequency range (typically 50 to 500 Hz). The large bandwidth of the shear wave generated through the ultrasonic radiation force allows this measurement in one shot.

Figure 4 shows a typical waveform of the shear velocity profile as a function of time at one given depth (Fig. 4a) and its corresponding frequency spectrum (Fig. 4b) in the liver. It appears that a large bandwidth can be exploited, from 50 to ~400 Hz.

The signal is first averaged over the depth of the ROI (15 mm depth in liver) to increase the signal ratio. Its Fourier transform is then computed and, for each frequency, the phase is extracted and unwrapped along the x axis. The last step consists in fitting the phase along the distance to retrieve the wave number k for each frequency. In Fig. 5a, only four phases (90 Hz, 120 Hz, 150 Hz and 180 Hz) as a function of depth are plotted to clarify the figure. In Fig. 5b, the frequency dispersion of the shear wave speed is illustrated by the phase information extracted from the spectrum of the local tissue displacement field as a function of the propagation distance. The slope of this phase function is changing with respect to the frequency component. Such a method could allow study of the full rheological behavior of the liver, through the assessment of the frequency dispersion of the shear wave speed. Using this approach, it was possible to perform a spectroscopic analysis in 10 of the 15 volunteers.

Experimental protocol

The objective of this study was (i) to demonstrate the feasibility of mapping elasticity of the liver through intercostal measurements *in vivo*, (ii) to assess the reproducibility of the shear velocity through intercostal measurements *in vivo*, (iii) to assess the repeatability of the shear velocity through intercostal measurements *in vivo*, (iv) to assess the interindividual variability of the shear velocity among a group of healthy volunteers and (v) to evaluate the benefit of shear wave spectroscopy in liver.

For each point of the objectives, the volunteers were asked to hold their breath during acquisition, and the ultrasonic device parameters were always the same. The mean body mass index was equal to 23.3 and values ranged from 19.2–29.3.

Reproducibility measurements were conducted by repeating 50 intercostal shear velocity measurements on one single volunteer, repositioning the probe between each measurement.

Repeatability measurements were conducted by repeating the same intercostal shear velocity measurement 50 times, without repositioning the probe, to increase the colocation of all measurements.

Reproducibility and repeatability measurements were performed using a single pushing line generated on the left of the B-mode image. A 15 × 25-mm ROI was

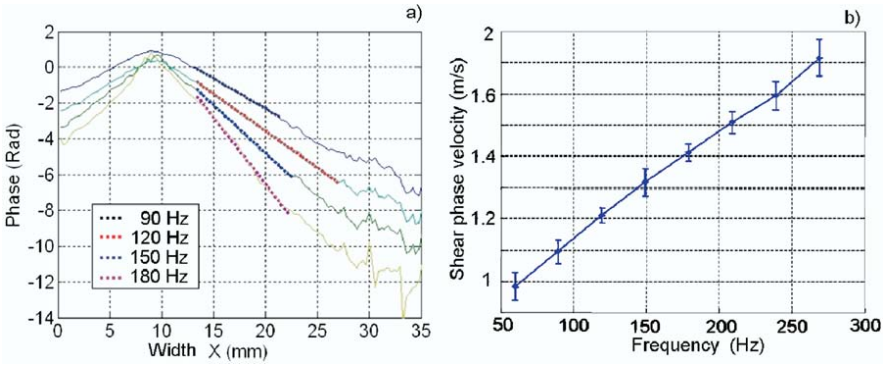

Fig. 5. (a) Four phases of the shear displacement for different frequencies (90 Hz, 120 Hz, 150 Hz and 180 Hz) as a function of distance (the width is the size of the transducer array). (b) Frequency dispersion of the shear wave speed calculated from the phases extracted between 60 Hz and 270 Hz.

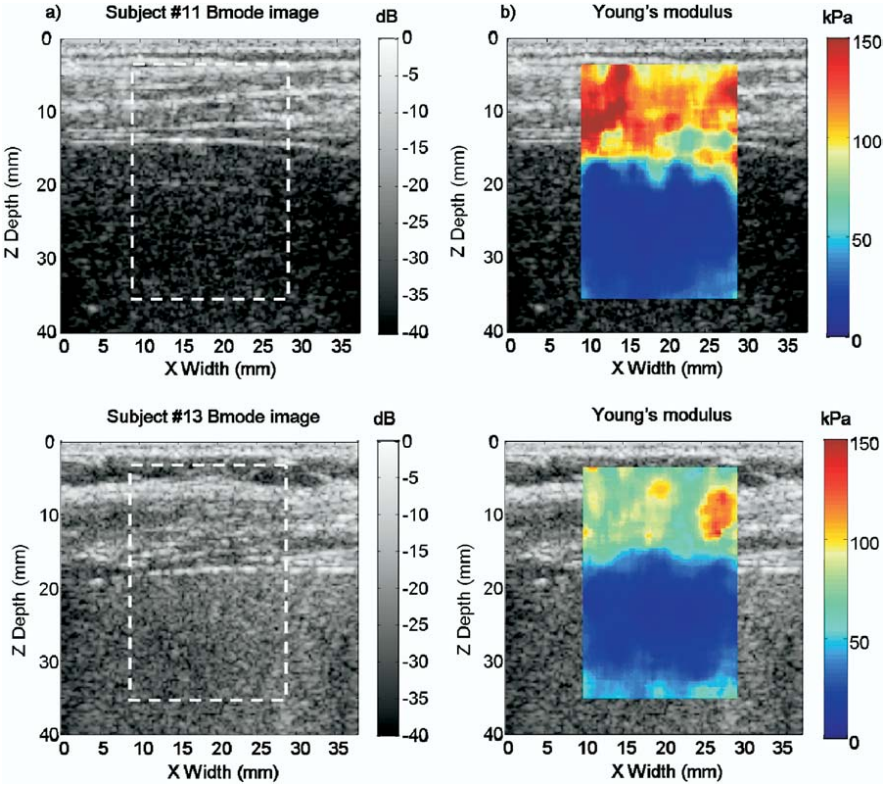

Fig. 6. Local shear velocity imaging in two healthy volunteers. (a) B-mode images of the liver for two healthy volunteers. (b) Mapping of the Young's modulus. The liver appears roughly four times softer than the intercostal muscle. One can also notice that both regions are homogeneous in terms of shear velocity.

used to evaluate the shear wave velocity in the middle of the B-mode image. So the sequence for these dispersion measurements was slightly different from the sequence used for elasticity imaging on the 15 volunteers. The same ROI was chosen for all measurements for the estimation of the global shear velocity.

In addition, intercostal liver shear velocity measurements were performed on 15 healthy volunteers using the supersonic shear imaging technique described above. Each imaging sequence was repeated five times. The ultrasonic probe was repositioned between each of the five reproducibility measurements. For each imaging sequence, three plane waves were generated on the left, center and right of the ROI to reduce the variance by averaging the velocity estimates and to provide a quantitative elasticity map over a large 40×40 mm^2 rectangular area.

For the repeatability/reproducibility experiment, the same protocol was used in terms of positioning the probe and controlling breathing (a 2-s breath-hold was asked of the volunteer for each acquisition). Regarding the sequences, the same parameters were used for mapping or assessing the repeatability/reproducibility measurement. The only difference between these two types of acquisitions was the number of pushing line (a pushing line corresponded to a set of 4 pushing beams at depth 20, 25, 30 and 35 mm) used. To map the entire region of the liver comprised in the B-mode image, three pushing lines were used: at the left, center and right of the image. For the repeatability/reproducibility experiment, only the left pushing line was used. Except this number of pushing lines, all other parameters were the same.

RESULTS

Imaging of local shear velocity on healthy volunteers

Shear velocity mapping results are presented for two healthy volunteers in Fig. 6, along with the corresponding B-mode images. Fat and muscle regions are well differentiated both in ultrasonographic and elasticity images. From the selected zone defined by the white rectangle on the B-mode image (Fig. 6a), the corresponding Young's modulus mapping is derived in Fig. 6b. Young's modulus appears almost homogeneous for a healthy volunteer in both liver and muscle regions. Mean shear velocity in the muscle region was found equal to 6.3 m/s, with a standard deviation of 1.2 m/s, whereas mean shear velocity in the liver region was found equal to 1.6 m/s, with a standard deviation of 0.15 m/s for subject 11. The higher standard deviation obtained in the

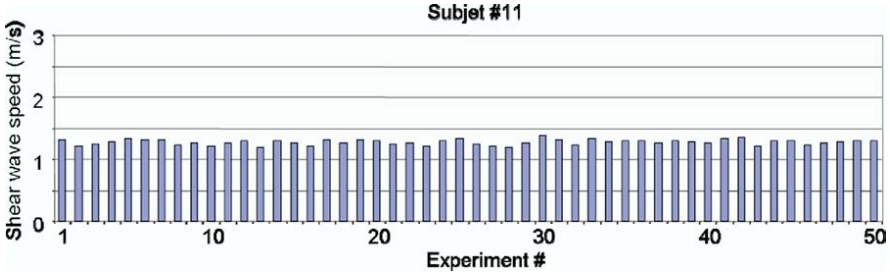

Fig. 7. Reproducibility measurement on a single healthy volunteer. The probe was removed and replaced on the abdomen of the subject and the subject held his breath between each acquisition. Standard deviation corresponds to 3.9 % of the mean value.

fat/muscle region is related to the higher heterogeneity of the region compared with the liver tissue.

Global group velocity estimation: reproducibility, repeatability and interindividual variability measurements on healthy volunteers

Figure 7 presents the shear group velocity distribution obtained from the reproducibility measurements (50 consecutive measurements with repositioning of the probe between each measurement) on a single healthy volunteer (subject 11). The volunteer was holding breath for 5 s to minimize any motion artifacts. The 50 measurements resulted in a mean group velocity value of 1.27 m/s (corresponding to a Young's modulus of 4.89 kPa), with a standard deviation of 0.05 m/s (corresponding to a 0.33 kPa standard deviation).

Results on repeatability are presented in Fig. 8. The repeatability measurements were performed by repeating 50 times the global shear wave speed on the same healthy volunteer (subject 11). The probe was maintained in the exact same position, and the subject held his breath during acquisition. The global velocity estimation obtained with this method resulted in a distribution with a mean value of 1.46 m/s (corresponding to a Young's modulus of 6.38 kPa) and a standard deviation of 0.04 m/s (corresponding to 0.37 kPa).

Furthermore global shear velocity was also assessed *in vivo* for a group of 15 healthy volunteers. Five measurements were conducted on each volunteer. Each measurement combined three plane waves: on the left, center and right of the ROI. The three velocity estimates were averaged to reduce the variability. The shear wave velocity distributions for all volunteers are presented in Fig. 9, along with the standard deviation of the measurements provided by the distribution of the five consecutive velocity measurements. The mean velocity value for the whole group of volunteers is 1.48 m/s (corresponding to a Young's modulus of 6.61 kPa), with a standard deviation of 0.16 m/s (respectively, 1.41 kPa).

Shear velocity dispersion estimation

In addition to the global shear velocity estimation, a much more refined study of the mechanical behavior of liver tissue can be conducted by estimating the frequency dependence (dispersion) of the shear phase velocity.

These dispersion curves were calculated for all 10 healthy volunteers in a large-frequency bandwidth. Interestingly, similar slopes were found for all volunteers for the phase velocity dispersion. Among all cases, the mean slope for the shear phase velocity dispersion was found to be 3.60 ± 0.82 mm (Fig. 10b). On Fig. 10, the three solid lines represent the F2, F3 and F4 scores defined by physicians at low frequency (Ziol et al. 2005) to characterize the liver fibrosis. The dashed lines represent the supposed evolution of these score at higher frequencies. Moreover, error measurements for these

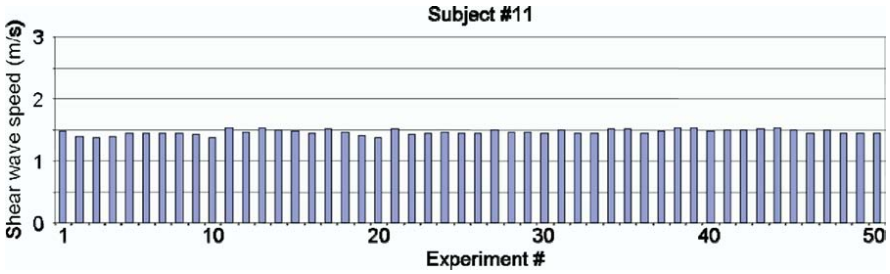

Fig. 8. Repeatability measurement on a single healthy volunteer. The probe was not moving and the subject held his breath during each acquisition. The standard deviation corresponds to 2.7% of the mean value.

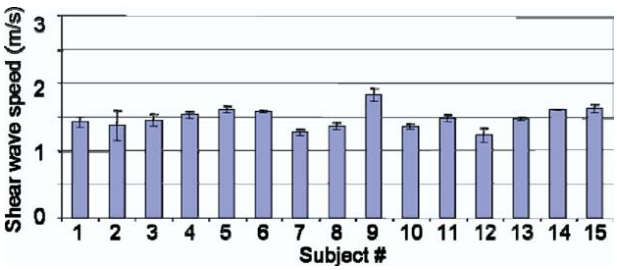

Fig. 9. Global shear group velocity estimation for 15 healthy volunteers. The error bars are the standard deviation calculated over 15 acquisitions. The probe was removed and replaced on the abdomen of the subject between all acquisitions.

shear velocity dispersion profiles were estimated by conducting reproducibility measurements of the shear velocity dispersion on a single volunteer (Fig. 10a). It resulted in a 0.38-mm error on the slope, smaller than the 0.82 mm standard deviation obtained for the studied population.

For volunteer 3, the median elasticity at 50 Hz is found to be $E = 3\rho c^2 = 4.42 \pm 0.64$ kPa. The median elasticity at 50 Hz (corresponding to the excitation frequency of Fibroscan©) is $E = 3\rho c^2 = 4.18 \pm 1.37$ kPa and is consistent with the results reported in the literature for a healthy group.

DISCUSSION

In this study, the feasibility of scanning viscoelastic properties of liver was investigated using the SSI technique on 15 healthy volunteers. Various liver characteristics have been estimated using different processes. Depending on the kind of required information (respectively, fibrosis staging or liver tumor imaging), it is possible to characterize global or local elastic properties of the liver.

Regarding global shear wave group velocity estimation, the SSI technique proved to be highly reproducible and repeatable (standard deviations equal, respectively, to 0.05 m/s [0.33 kPa] and 0.04 m/s [0.37 kPa] for 50 consecutive measurements). These low standard deviations foretell a very low measurement error (typically 6% of the mean Young's modulus), and therefore a particularly strong accuracy of the measurement. Using the SSI mode, the standard deviation on the estimated Young's modulus is smaller (at least three times smaller) than the ones obtained by the ARFI approach reported in Palmeri et al. (2008). Regarding the mean velocity values of the reproducibility and repeatability measurements, a difference of 0.19 m/s is noticeable on the same subject. This could be explained by three points. First, the assessments were not done the same days. Second, the position of the probe for the repeatability and the reproducibility measurements was probably not the same. The probe was placed between the same two ribs as close as possible at the same distance from the abdominal part, so it was not precisely the same part of the liver investigated, which could have some weak heterogeneity. Finally, the positioning of the probe between the ribs is crucial and could generate some biases. The intercostal space can lead to ultrasonic beam aberrations. Such aberrations and absorption effects on the ultrasonic beam could also have a slight impact on the bandwidth of the generated shear wave (which is linked to the ultrasonic beam shape). As liver tissue is dispersive, a change in the shear wave bandwidth could also lead to slight changes in the shear wave group velocity.

Nevertheless, good accuracy should be a *sine qua non* condition to discriminate pathologic states *via* elas-

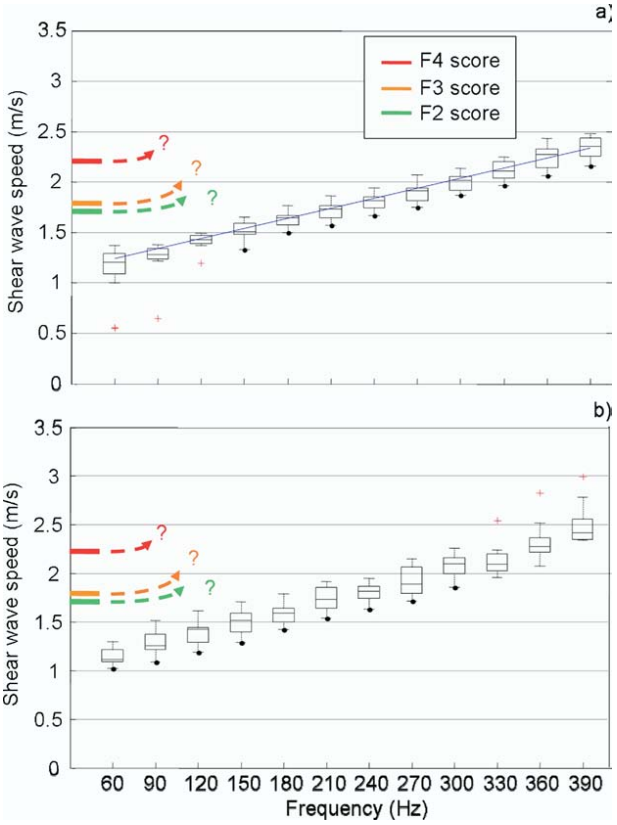

Fig. 10. (a) Repeatability of the dispersion curves for volunteer 3. The box and whiskers diagram was computed over 10 repeated measurements and are minimum in the 60–390 Hz range. The slope is 3.30 ± 0.38 mm and the extrapolated values at 50 Hz are 1.21 ± 0.09 m/s, indicating an F0 score. (b) Shear phase velocity dispersion for 10 healthy volunteers. Interestingly, the slope is in the same range for all volunteers and around 3.60 ± 0.82 mm, and the extrapolated values at 50 Hz are 1.18 ± 0.18 m/s, also indicating an F0 score for the group. Thresholds on the right correspond to the fibrosis scores estimated using Fibroscan© and so provided at 50 Hz only (Ziol et al. 2005). It does not mean that these thresholds are the same at higher frequencies, as suggested by the arrows.

ticity measurements that are very close at early stages of liver fibrosis as shown by Huwart et al. (2006). In particular, for a 50-Hz mechanical excitation, F0–F2 stages, characterizing the transition from normal to the first pathologic stage, are confined in a short range of Young's moduli (from 3.35 to 7.60 kPa), corresponding to close shear velocities (from 1.06 to 1.59 m/s) (Sandrin et al. 2003). Because MR-elastography benefits from much more accurate estimations than Fibroscan© at the same excitation frequency (50 Hz), it permits to distinguish F0–F2 and F3 stages (Salameh et al. 2008).

Interestingly, the shear group velocities assessed in 15 healthy volunteers using our SSI approach were found to be larger (mean value 1.48 ± 0.16 m/s) than the average value usually measured with clinical tools such as Fibroscan©. Indeed, at the F0 and F1 stages of fibrosis, the Fibroscan© measurement provides an elasticity of roughly 3.35 kPa and 5.10 kPa (Sandrin et al. 2003) (corresponding to shear velocity of 1.06 m/s and 1.30 m/s), whereas a mean value of 6.57 kPa was found using the SSI modality. This elasticity gap is a result of the broadband characteristic of the mechanical excitation generated using the ultrasonic radiation force of the SSI mode. As presented in Fig. 4, the shear wave velocity is estimated over a much larger frequency bandwidth, and *in vivo* liver tissues are demonstrated to be very dispersive in that 50–350 Hz frequency range. Thus, high-frequency components of the shear wave propagate much faster than lower ones. The shear phase velocity dispersion relation obtained demonstrates that the shear velocity increases with frequency (Fig. 5b). Thus, liver elasticity is probed in a higher frequency range than Fibroscan© (50 Hz) or MR-elastography (51 Hz) (Klatt et al. 2006). An increased global elasticity was, therefore, expected using such a higher spectral content and this point was confirmed experimentally. These results are of particular interest because they emphasize the ability of this new SSI modality to provide additional information compared with Fibroscan© or MR-elastography: the full mechanical response of liver tissues over a large bandwidth of mechanical excitation. To provide a comparison with the state-of-the-art values provided by MR-elastography and Fibroscan©, a linear fit of the shear wave velocity dispersion curve was performed for each healthy volunteer, from which the shear wave velocity at 50 Hz was extracted. The shear wave velocity estimated at 50 Hz was found to be 1.18 ± 0.18 m/s for the volunteer group (corresponding to Young's modulus equal to 4.18 ± 1.37 kPa). In addition to a very small variance of these estimates, these values are in agreement with the data provided in the literature. Thus, the broadband feature of the SSI modality permits to estimate elasticity values at a low excitation frequency corresponding to the other clinical approaches, but additionally provides new information in a wider and higher frequency range.

An interesting result concerns the good reproducibility of the shear velocity dispersion for each single healthy volunteer. The assessment of the frequency slope of shear wave velocity for a volunteer resulted in a 16% variability (mean shear velocity dispersion value: 3.30 mm, standard deviation: 0.38 mm). More interestingly, for all healthy volunteers, similar shear dispersion behavior was observed. Frequency slopes of the shear wave dispersion were estimated for each volunteer, and a 20% variation was obtained for the whole population (mean shear velocity dispersion value: 3.60 mm, standard deviation: 0.82 mm) (Fig. 10b). Further work will be required to determine if the assessment of these dispersion parameters (linked to shear viscosity) will represent an added value for the diagnostics of pathologic liver diseases. However, it is possible that this type of parameter could provide interesting information on tissue organization at the microscopic level. Ongoing work is investigating this assumption. It has been demonstrated in this study that the rheological behavior of the liver can be estimated locally over a large bandwidth of mechanical excitation. Dispersion curves estimated for all healthy volunteers give elasticity values at 50 Hz that are in total agreement with narrowband approaches (MR-elastography and Fibroscan©). At this particular frequency, all healthy volunteers were in the F0–F1 region as defined by state of the art (Ziol et al. 2005; Pinzani et al. 2005). It would be extremely interesting to study the frequency dependence of these fibrosis scores boundary values. In particular, the elasticity values provided for the F2/F3 differentiation using MR-elastography and Fibroscan© are extremely close at 50 Hz. A clinical evaluation of shear wave spectroscopy for fibrosis staging should be conducted to estimate the evolution of these boundary elasticity values at higher frequencies, because it is anticipated that differentiation could be better at higher frequencies. Finally, different regions with a typical size of some millimeters can be estimated independently. The influence of the size of the selected region for the spectroscopic analysis is carefully studied in the paper by Deffieux et al. (2008). This is therefore a very promising step toward the full mapping of the rheological properties of the liver.

Additionally, to such local shear wave spectroscopy a simplified approach can be used by estimating the local elasticity through a straightforward time-of-flight algorithm, leading to the determination of elasticity maps with a millimeter resolution. For such an imaging approach, the Young's modulus estimation is not as refined as in the previous spectroscopy case because the time-of-flight algorithm provides a shear group velocity corresponding to an averaged value in the case of a disper-

sive medium. The Young's modulus estimate corresponds to the value of the shear modulus at the central frequency of our broadband radiation force excitation. Results presented in Fig. 6, obtained on healthy volunteers, show that it is possible to discriminate higher elasticity regions such as the muscle regions. Such quantitative elasticity mapping could provide very useful information on the pathologic state of the liver *via* stiffness heterogeneity, as well as provide information on the presence of tumors.

Some technical limitations encountered during this feasibility study could be overcome to improve the results. One of the limitations of this study relies on the fact that *in vivo* experiments were conducted using a linear transducer array, implying that the full organ could not be scanned. Subcostal measurements were hard to perform using such a linear array because of the limited imaging depth. To improve this discrepancy, a curved array working at a lower ultrasonic frequency (~3 MHz) should be considered. This implies additional work because it requires the implementation of the ultrafast echographic modality for a curved array. Such easy technical improvements should considerably help for subcostal liver imaging to cover the full size of the liver.

Finally, one of the particularly interesting aspects of the SSI technique relies in its ultrafast imaging characteristics. The ability to reach frame rates up to 5000 frames/s removes the influence of the low-frequency displacements artefacts, such as respiratory motion or cardiac vibrations, which tend to degrade other approaches (Fahey et al. 2006, 2007). No significant influence of motion artefacts were seen during ultrafast acquisitions.

CONCLUSION

Quantitative mapping of liver tissue viscoelasticity is feasible *in vivo* using the SSI approach. By combining the use of ultrafast echographic imaging and the generation of remote and in-depth palpations using the acoustic radiation force induced by the echographic probe, it enables the overcoming of many limitations of elastographic techniques for liver applications. On the one hand, it is insensitive to respiratory motion artefacts. On the other hand, the generation of shear waves can be achieved in depth and consequently are not influenced by liquid barriers. Using the intercostal window, the SSI mode is able to generate shear wave fronts propagating through several centimeters of liver tissue and to monitor these shear waves *via* an ultrafast acquisition capability. Quantitative shear elasticity images were obtained *in vivo* on 15 healthy volunteers and a clear delineation between the Young's modulus value derived from shear group velocity for intercostal muscle ($E \approx 100$ kPa) and normal liver ($E < 10$ kPa) is obtained. Elasticity images obtained in healthy volunteers are found to be quite homogeneous as expected and corresponding values are consistent with the literature. Moreover, a global mean elasticity of liver for fibrosis staging can be provided by averaging elasticity maps over very large areas (>10 cm^{-2}). This estimation of this mean elasticity value is shown to be very repeatable and reproducible in healthy volunteers. Finally, the assessment of the mechanical behavior of liver tissues over quite a large bandwidth (typically 50 to 400 Hz) *via* the shear wave dispersion can be achieved *in vivo*, paving the way to a shear wave spectroscopy of liver tissues. This feasibility study clearly emphasizes the potential of the SSI approach for liver viscoelasticity imaging and the interest of a future clinical investigation.

REFERENCES

Afdhal NH. Diagnosis fibrosis in hepatitis C: Is the pendulum swinging from biopsy to blood tests? Hepatology 2003;37:972–974.

Aguirre DA, Behling CA, Alpert E, Hassanein TI, Sirlin CB. Liver fibrosis: Noninvasive diagnosis with double contrast material-enhanced MR imaging. Radiology 2006;239:425–437.

Bataller R, Brenner DA. Liver fibrosis. J Clin Invest 2005;115:209–218.

Beaugrand M. How to assess liver fibrosis and for what purpose? J Hepatol 2006;44:444–445.

Bedossa P, Poynard T, Naveau S, Martin ED, Agostini H, Chaput JC. Observer variation in assessment of liver biopsies of alcoholic patients. Alcohol Clin Exp Res 1988;12:173–178.

Bercoff J, Tanter M, Muller M, Fink M. The role of viscosity in the impulse diffraction field of elastic waves induced by the acoustic radiation force. IEEE Trans Ultrason Ferroelectr Freq Control 2004a;51:1523–1536.

Bercoff J, Tanter M, Fink M. Sonic boom in soft materials: The elastic Cerenkov effect. Appl Phys Lett 2004b;84(12):2202–2204.

Bercoff J, Tanter M, Fink M. Supersonic shear imaging: A new technique for soft tissues elasticity mapping. IEEE Trans Ultrason Ferroelectr Freq Control 2004c;51(4):396–409.

Bravo AA, Sheth SG, Chopra S. Liver biopsy. N Engl J Med 2001; 344:495–500.

Cadranel JF, Rufat P, Degos F. Practices of liver biopsies in France: Results of a prospective nationwide survey. For the Group of Epidemiology of the French Association for the Study of the Liver. Hepatology 2000;37:477–481.

Castera L, Negre I Samii K, Buffet C. Pain experienced during percutaneous liver biopsy. Hepatology 1999;30:1529–1530.

Castera L, Vergniol J, Foucher J, Brigitte Le Bail B, Chanteloup E, Haaser M, Darriet M, Couzigou P, de Lédinghen V. Prospective comparison of transient elastography, Fibrotest, APRI, and liver biopsy for the assessment of fibrosis in chronic hepatitis C. Gastroenterology 2005;128:343–350.

Deffieux T, Montaldo G, Tanter M, Fink M. Shear wave spectroscopy for in vivo quantification of human soft tissues viscoelasticity. IEEE Trans Med Imaging 2008; in press.

Fahey BJ, Nelson RC, Bradway DP, Hsu SJ, Dumont DM, Trahey GE. In vivo visualization of abdominal malignancy with acoustic radiation force elastography. Phys Med Biol 2008;53:279–293.

Fahey BJ, Palmeri ML, Trahey GE. The impact of physiological motion on tissue tracking during radiation force imaging. Ultrasound Med Biol 2007;33:1149–1166.

Fahey BJ, Palmeri ML, Trahey GE. Frame rate considerations for real-time abdominal acoustic radiation force impulse imaging, Ultrason Imaging 2006;28:193–210.

Friedman SL. Liver biopsies, from bench to bedside. J Hepatol 2003; 38(suppl1):S38–S53.

Friedrich-Rust M, Ong MF, Herrman E, Dries V, Samaras P, Zeuzem S, Sarrazin C. Real-time elastography for noninvasive assessment of liver fibrosis in chronic viral hepatitis. AJR Am J Roentgenol 2007;188:758–764.

Huwart L, Peeters F, Sinkus R, Annet L, Salameh N, ter Beek LC, Horsmans Y, Van Beers BE. Liver fibrosis: non-invasive assessment with MR-elastography. NMR Biomed 2006;19:173–179.

Imbert-Bismut F, Ratziu V, Pieroni L, Charlotte F, Benhamou Y, Poynard T. Biochemical markers of liver fibrosis in patients with hepatitis C virus infection: A prospective study. Lancet 2001;357: 1069–1075.

Ishak K, Baptista A, Bianchi L, Callea F, De Groote J, Gudat F, Denk H, Desmet V, Korb G, MacSween RN, Phillips MJ, Portmann BG, Poulsen H, Scheuer PJ, Schmid M, Thaler. Histological grading and staging of chronic hepatitis. J Hepatol 1995;22:696–699.

Klatt D, Asbach P, Rump J, Papazoglou S, Somasunaram R, Modrow J, Braun J, Sack I. In vivo determination of hepatic stiffness using steady state free precession magnetic resonance elastography. Invest Radiol 2006;42:841–848.

Konig CW, Trubenbach J, Fritz J. Contrast enhanced MR-guided biopsy of hepatocellular carcinoma. Abdom Imaging 2004;29:71–76.

Maharaj B, Maharaj RJ, Leary WP, Cooppan RM, Naran AD, Pirie D, Pudifin DJ. Sampling variability and its influence on the diagnostic yield of percutaneous needle biopsy of the liver. Lancet 1986;1: 523–525.

National Institute of Health Consensus Development Conference Statement. Management of Hepatitis C: June 2002. Hepatology 2002; 36[5 suppl 1]:S3–S20.

Ono E, Shiratori Y, Okudaira T, Imamura M, Teratani T, Kanai F, Kato N, Yoshida H, Shiina S, Omata M. Platelet count reflects stage of chronic hepatitis C. Hepatol Res 1999;15:192–200.

Ophir J, Cespedes I, Ponnekanti H, Yazdi Y, Li X. Elastography: A quantitative method for imaging the elasticity of biological tissues Ultrason Imaging 1991;13(2):111–134.

Palmeri ML, Wang MH, Dahl JJ, Frinkley KD, Nightingale KR. Quantifying hepatic shear modulus in vivo using acoustic radiation force. Ultrasound Med Biol 2008;34:546–558.

Patel K, Lajoie A, Heaton S, Pianko S, Behling C, Bylund D, Pockros P, Blatt L, Conrad A, Mchutchison J. Clinical use of hyaluronic acid as a predictor of fibrosis change in hepatitis C. J Gastroenterol Hepatol 2003;18:253–257.

Pinzani M, Rombouts K, Colagrande S. Fibrosis in chronic liver diseases: Diagnosis and management. J Hepatol 2005;42:S22–S36.

Regev A, Berho M, Jeffers LJ, Milikowski C, Molina EG, Pyrsopoulos NT, Feng ZZ, Reddy KR, Schiff ER. Sampling error and intraobserver variation in liver biopsy in patients with chronic HCV infection. Am J Gastroenterol 2002;97:2614–2618.

Royer D, Dieulesaint E. Elastic waves in solids, vol. 1. Springer-Verlag, 2000.

Saito H, Tada S, Nakamoto N, Kitamura K, Horikawa H, Kurita S, Saito Y, Iwai H, Ishii H. Efficacy of non-invasive elastometry on staging of hepatic fibrosis. Hepatol Res 2004;29:97–103.

Sandrin L, Fourquet B, Hasquenoph JM, Yon S, Fournier C, Mal F, Christidis C, Ziol M, Poulet B, Kazemi F, Beaugrand M, Palau R. Transient elastography: A new non-invasive method for assessment of hepatic fibrosis. Ultrasound Med Biol 2003;29:1705–1713.

Sarvazyan AP, Rudenko OV, Swanson SD, Fowlkes JB, Emelianov SY. Shear wave elasticity imaging: A new ultrasonic technology of medical diagnostics. Ultrasound Med Biol 1998;24(9):1419–1435.

Stauber RE, Lackner C. Noninvasive diagnosis of hepatic fibrosis in chronic hepatitis C. World J Gastroenterol 2007;13(32):4287–4294.

Suzuki A, Angulo P, Lymp J, Li D, Satomura S, Lindor K. Hyaluronic acid, an accurate serum marker for severe hepatic fibrosis in patients with non-alcoholic fatty liver disease. Liver Int 2005;25:779–786.

Tanter M, Bercoff J, Athanasiou A, Deffieux T, Gennisson J-L, Montaldo G, Muller M, Tardivon A, Fink M. Quantitative assessment of breast lesion viscoelasticity: Initial clinical results using supersonic shear imaging. Ultrasound Med. Biol 2008;34.

The French METAVIR Cooperative Study Group. Intraobserver and interobserver variations in liver biopsy interpretations in patients with chronic hepatitis C. Hepatology 1994;20:15–20.

Wai, CT, Greenson JK, Fontana RJ, Kalbfleisch JD, Marrero JA, Conjeevaram HS, Lok AS. A simple noninvasive index can predict both significant fibrosis and cirrhosis in patients with chronic hepatitis C. Hepatology 2003;38:518–526.

Yeh WC, Li PC, Jeng YM, Hsu HC, Kuo PL, Li ML, Yang PM, Lee PH. Elastic modulus measurements of human liver and correlation with pathology. Ultrasound Med Biol 2002;28(4):467–474.

Ziol M, Handra-Luca A, Kettaneh A, Christidis C, Mal F, Kazemi F, de Lédinghen V, Marcellin P, Dhumeaux D, Trinchet JC, Beaugrand M. Noninvasive assessment of liver fibrosis by measurement of stiffness in patients with chronic hepatitis C. Hepatology 2005;41: 48–54.